Formation of fibrillar structures through self-assembly of designed peptide turns

Sudeshna Kar,[a] Michael G. B. Drew,[b] and Animesh Pramanik[a,*]

[a] *Department of Chemistry, University of Calcutta, 92, A. P. C. Road, Kolkata-700 009, India*
[b] *School of Chemistry, The University of Reading, Whiteknights, Reading RG6 6AD, UK*
E-mail: animesh_in2001@yahoo.co.in

Abstract

Three tripeptides Boc-Phe-Aib-Val-OMe (**1**), Boc-Leu-Aib-*p*-NA-NO_2 (**2**) and Boc-Pro-Aib-*m*-NA-NO_2 (**3**) (Aib: α-aminoisobutyric acid; *p*- and *m*-NA: *para*- and *meta*-nitroaniline) have been designed by incorporating aromatic rings to study the self-assembly and fibril formation. Single crystal X-ray diffraction studies show that all the peptides adopt turn-like structures that are self-assembled through intermolecular hydrogen bonds and van der Waals interactions to create layers of β-sheets. Solvent dependent NMR titration and CD studies show that the turn structures of the peptides also exist in the solution phase. The field emission scanning electron microscopic (FE-SEM) images of the peptides in the solid state reveal fibrillar structures of flat morphology that are formed through β-sheet mediated self-assembly of the preorganized turn building blocks.

Keywords: Peptides, turns, self-assembly, β-sheet, fibrils

Introduction

The design and synthesis of appropriate peptide subunits for desired supramolecular architecture is an important area of current research. Supramolecular helices[1,2] and β-sheets[3] are the most common supramolecular architectures derived from peptides through self-assembly. Supramolecular β-sheets have many potential applications in material[4-7] as well as in biological sciences.[8-11] Amyloid fibril forming β-sheets are the causative factors of many neurodegenerative diseases.[12,13] It has been observed that a β-turn subunit can either form a supramolecular β-sheet or a supramolecular helix through self-assembly.[14-17] In this paper we are interested in designing small synthetic peptides that exhibit turn structures, and have the potential to form supramolecular β-sheets through molecular self-assembly.

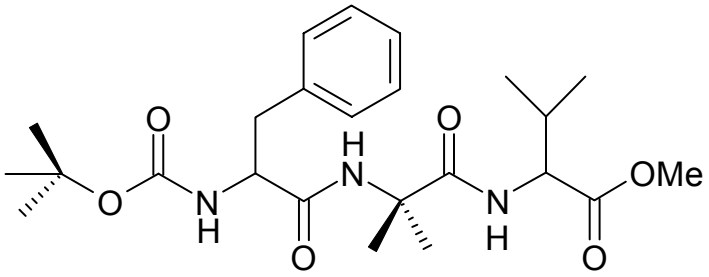

Peptide **1**

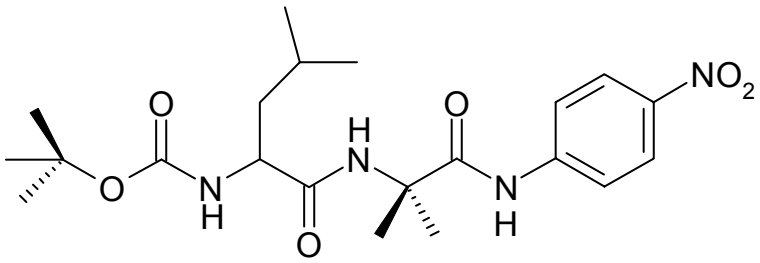

Peptide **2**

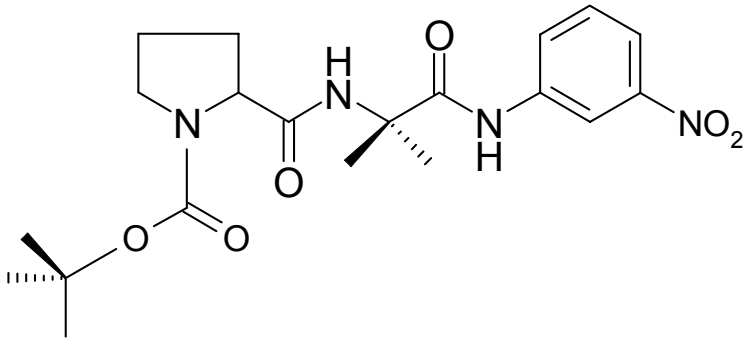

Peptide **3**

Figure 1. Schematic representation of peptides **1**-**3**.

Three model tripeptides Boc-Phe-Aib-Val-OMe (**1**), Boc-Leu-Aib-*p*-NA-NO_2 (**2**) and Boc-Pro-Aib-*m*-NA-NO_2 (**3**) (Aib: α-aminoisobutyric acid; *p*- and *m*-NA: *para*- and *meta*-nitroaniline) with a centrally placed non-coded amino acid Aib have been chosen to study the self-assembly and fibril formation (Fig. 1). Since it is well established that short aromatic peptides have the ability to form β-sheet mediated amyloid fibrils,[18] peptides **1**-**3** have been designed incorporating aromatic rings. While peptide **1** contains an aromatic ring in the side chain, peptide **2** and **3** incorporate aromatic rings in the backbone. Generally conformationally restricted Aib is a β-sheet breaker and highly helicogenic.[19] Therefore peptides **1**-**3** with a centrally positioned Aib(2) are expected to adopt turn-like structures.[20-22] It will be interesting to know whether the incorporation of *p*- and *m*-nitroanilnes in peptide **2** and **3** assists or disrupts the

creation of turn structures. There are examples of constrained cyclic peptides in which substituted benzenes have been inserted to mimic the turn region of the neurotrophin, a nerve growth factor.[23] Peptide **2** and **3** will be examples of acyclic analogues if they adopt turn-like structures. The present study will also reveal the influence of aromatic rings in self-assembly, specially in the formation of supramolecular β-sheets and fibrillar structures. Peptides **1**-**3** were synthesized using conventional solution phase methodology and their solid-state structures and crystal packing were determined by X-ray diffraction analyses. The peptide conformations in the solution phase were probed by CD and NMR studies. Field emission scanning electron microscopy (FE-SEM) has been employed to investigate the morphological properties of the peptides in the solid state.

Results and Discussion

Crystal structures of peptides

Peptide **1** crystallizes in spacegroup $P2_1$ with two molecules **1A** and **1B** in the crystallographic asymmetric unit. The structure of the two molecules is shown in Figure 2 and it is apparent that the two molecules for the most part conform to centrosymmetric pairs, indeed the majority of the coordinates fit to spacegroup $P2_1/c$. The chirality at C(4A) is *R* and at C(4B) is *S* but the symmetry is broken by C(10A) and C(10B) which both have chirality *S* which conformed with the starting material. During the synthesis it is clear that epimerization has occurred at Phe of molecule **1A** to produce molecule **1B** with opposite chirality at C(4). However the main conformational features of the two molecules are similar. Thus **1A** reveals a type II' β-turn-like structure with Phe(1) and Aib(2) occupying the $i + 1$ and $i + 2$ positions respectively (Fig. 2). The torsion angles at Phe(1) and Aib(2) were found to φ_1: 66.8(2), ψ_1 : -146.3(2)^o and φ_2 : -60.0(2), ψ_2 : -37.6(2)^o, respectively (Table 1), which deviate significantly from the ideal values for a type II' β-turn φ_1: 60, ψ_1 : -120 and φ_2 : -80, ψ_2 : 0.[24] The molecule **1B**, where the Phe has *S* chirality, adopts a type II β-turn-like structure, diastereomeric to **1A**, with Phe(1) and Aib(2) as corner residues (Fig. 2 and Table 1). The torsion angles at Phe(1) and Aib(2) were found to φ_1: -61.3(2), ψ_1 : 144.7(2)^o and φ_2 : 54.6(2), ψ_2 : 37.8(2)^o, respectively. In **1B**, the observed N(3B)...O(9B) distance between the Boc-CO and Val(3)-NH groups is far too long at 3.61(1)Å for an intramolecular 4→ 1 hydrogen bond. Importantly such turn-like structures, which do not contain intramolecular hydrogen bonds are solely stabilized by co-operative steric interactions amongst the amino acids residues and are generally referred to as open turns.[25]

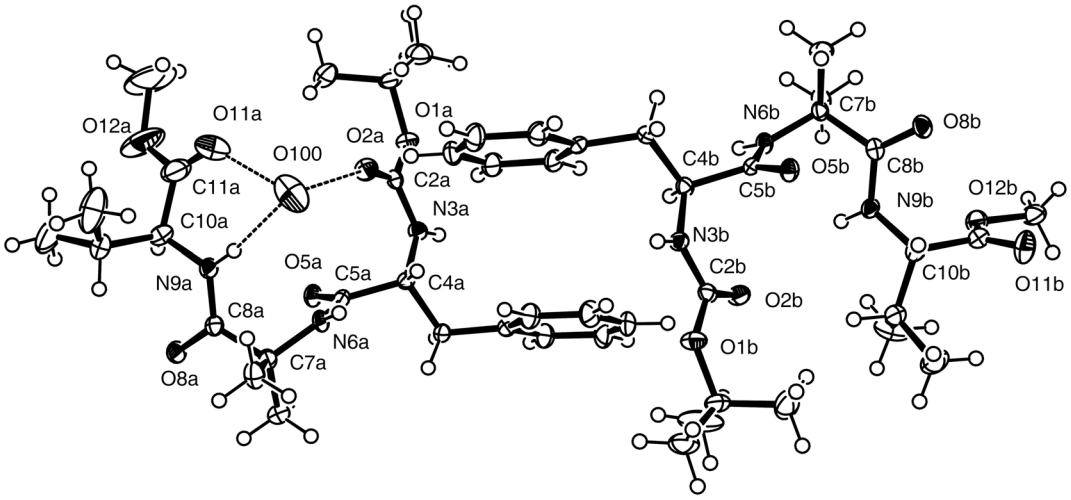

1A **1B**

Figure 2. ORTEP diagram of peptide **1** (**A** & **B**) with atom numbering scheme showing the pseudo centre of symmetry broken at C(10). Ellipsoids at 50% probability. Hydrogen bonds are shown as dotted lines.

Table 1. Selected back-bone torsion angles (°) for the peptides **1-3**

Peptide	Residue	ϕ	ψ	ω
1A	Phe(1)	66.8(2)	-146.3(2)	-158.9(2)
	Aib(2)	-60.0(2)	-37.6(2)	177.2(2)
	Val(3)	-158.9(2)	162.8(2)	
1B	Phe(1)	-61.3(2)	144.7(2)	167.5(2)
	Aib(2)	54.6(2)	37.8(2)	-168.5(2)
	Val(3)	-63.1(2)	-37.8(2)	
2	Leu(1)	-62.9(4)	143.1(3)	168.7(3)
	Aib(2)	63.5(4)	23.4(4)	179.0(4)
3	Pro(1)	-48.2(3)	133.5(2)	173.1(2)
	Aib(2)	66.1(3)	18.6(3)	168.6(2)

However in **1A**, a water molecule, O(100) is found within the cavity formed by the turn structure, albeit with 50% probability, and this solvent molecule forms three hydrogen bonds, as donor to O(11A) at 2.652(6)Å and O(2A) at 2.753(4)Å and acceptor from N(9A)-H(9A) at 3.039(5)Å. As a consequence the N(3A)...O(9A) distance is extended even longer than the N(3B)...O(9B) distance at 4.22(1)Å. There are additional intermolecular hydrogen bonds involving N(3)-H and N(6)-H in both molecules with carbonyls O(5) and O(8) (Table 2). On the other hand N(9A)-H only forms a hydrogen bond with the solvent O(100), while N(9B)-H is unattached.

Peptide **2** crystallizes in the centrosymmetric spacegroup Pbcn thus contains the two diastereomers with type II and II' β-turn-like conformations, with Leu(1) and Aib(2) as corner residues (Fig. 3, Table 1). The torsion angles at Leu(1) and Aib(2) were found to φ_1: -62.9(4), ψ_1 : 143.1(2)^o and φ_2 : 63.5(4), ψ_2 : 23.4(4)^o respectively, similar to those in peptide **1**. As in **1A** and **1B**, the conformation does not allow for a strong intramolecular 4→ 1 hydrogen bond between *p*-NA-NH and Boc-CO with N(9)...O(2) 3.66(1)Å (Table 2). However as in **1**, N(3)-H(3) forms a hydrogen bond with O(5)(1-x,1-y, -z) at 2.912(3)Å and N(6)-H(6) with O(8) (1.5-x, 0.5+y, z) at 2.934(3)Å while N(9)-H(9) remains unattached unless the weak intramolecular interaction with O(2) is considered.

The crystal structure of the peptide Boc-Pro-Aib-*m*-NA-NO_2 (**3**) is determined in the non-centrosymmetric spacegroup $P2_12_12$. While the chirality was not determined from the crystal structure determination, the enantiomer with C(4) having the *S* chirality was selected to conform with the reactant. The structure reveals a turn-like structure similar to that found in peptide **1** and **2** with Pro(1) and Aib(2) occupying the $i + 1$ and $i + 2$ positions respectively (Fig. 4). The torsion angles at the corner residues Pro(1) and Aib(2) are found to be as φ_1: -48.2(3)^o, ψ_1 : 133.5(2)^o and φ_2 : 66.1(3)^o, ψ_2 : 18.6(3)^o, respectively, indicating a type II β-turn structure (Table 1). The turn structure is stabilized by a 4→ 1 hydrogen bond between *m*-NA-NH and Boc-CO with the N9…O2 distance at 3.075(2) Å, very much shorter than the equivalent distance in **1** and **2** (Table 2).

Table 2. Hydrogen bonds parameters for peptides **1-3**

Type	N....O/(Å)	H....O/(Å)	O....H-N/(°)
Peptide 1A			
N3(A)-H3(A)....O(5B)[a]	2.905(2)	2.08	160
N(6A)-H(6A)...O(8A)[b]	2.849(2)	2.26	125
N9(A)-H9(A)....O(100)	3.039(5)	2.19	172
O(100)*...O(2A)	2.753(4)		
O(100)*...O(11A)	2.652(6)		
Peptide 1B			
N(3B)-H(3B)...O(5A)[c]	2.948(2)	2.08	156
N(6B)-H(6B)...O(8B)[d]	2.937(2)	2.26	135
Peptide 2			
N(3)-H(3)...O(5)[e]	2.912(3)	2.09	160
N(6)-H(6)....O(8)[f]	2.934(3)	2.07	166
Peptide 3			
Intramolecular			
N(9)-H(9)....O(2)	3.075(2)	2.29	151
Intermolecular			
N(6)-H(6)....O(8)[g]	2.930(2)	2.08	172

Symmetry elements: [a] x,1+y, z; [b] 1-x, y-0.5, 2-z; [c] x, y-1, z; [d] 1-x, y+0.5, 1-z; [e]1-x, 1-y, -z; [f]1.5-x, 0.5+y, z; [g] x, y, 1+z.

* Hydrogen atoms on the water molecule O(100) were not located.

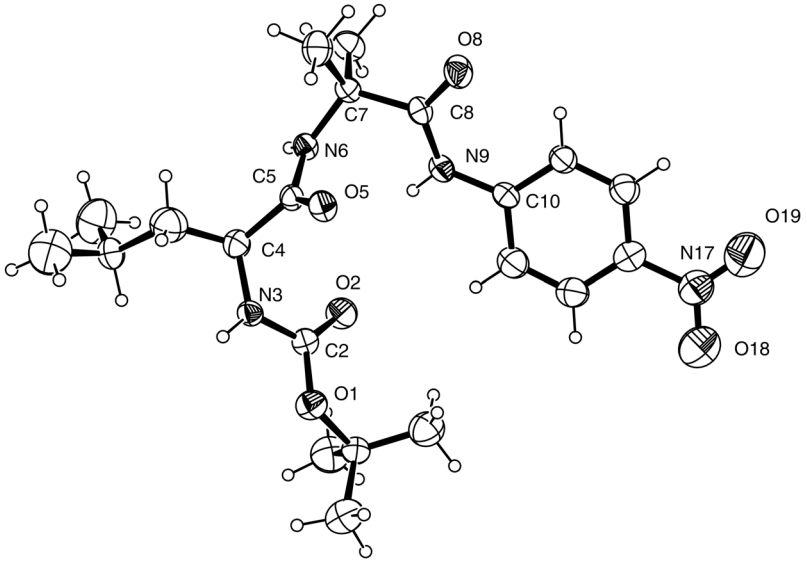

Figure 3. ORTEP diagram of peptide **2** with atom numbering scheme. Ellipsoids at 50% probability.

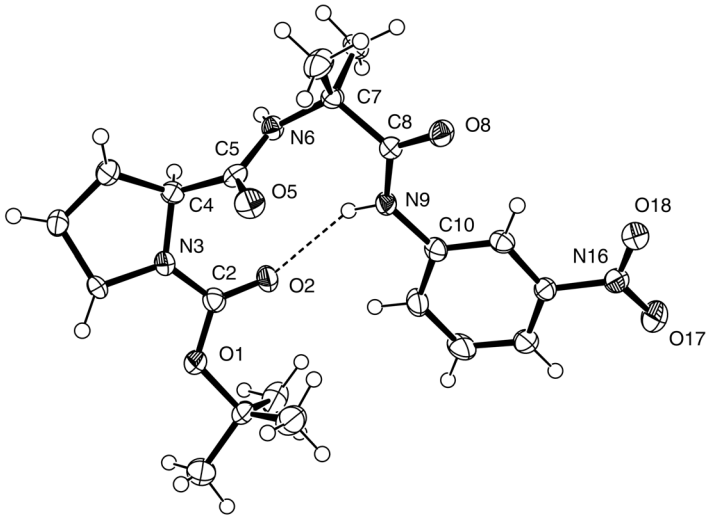

Figure 4. ORTEP diagram of peptide **3** with atom numbering scheme. Ellipsoids at 50% probability. Hydrogen bond as dotted line.

Crystal packing of peptides

Crystal structure analysis shows that the turn structures of peptides **1** and **2** are packed in a similar fashion to form layers of β-sheets (Fig. 5 and 6). In each case six peptide molecules are interconnected by two types of intermolecular hydrogen bonds Xx(1)-CO…NH-Xx(1) and Aib(2)-CO…NH-Aib(2) to complete each circular subunit (Fig. 5a & 6a, Table 2). These circular

subunits are interconnected to create layers of β-sheets such as *ac* plane for peptide **1** and *bc* plane for peptide **2**. The layer structures of the peptides are further self-assembled along the crystallographic directions *b* (for **1**) and *a* (for **2**) *via* van der Waals interactions to form higher order supramolecular β-sheet structures (Fig. 5b & 6b). In the case of peptide **3**, the intermolecular hydrogen bond Xx(1)-CO…NH-Xx(1) does not exist as the Pro(1) residue does not provide a suitable proton. The only hydrogen bond Aib(2)-CO…NH-Aib(2) connects the molecules of **3** in the *b* direction to form semicylindrical structures, which are packed through van der Waals interactions to create layers of β-turns in the *ac* plane (Fig. 7). Therefore all the peptides **1**-**3** create β-sheet-like structure through molecular self-assembly, consistent with the previous results.[17]

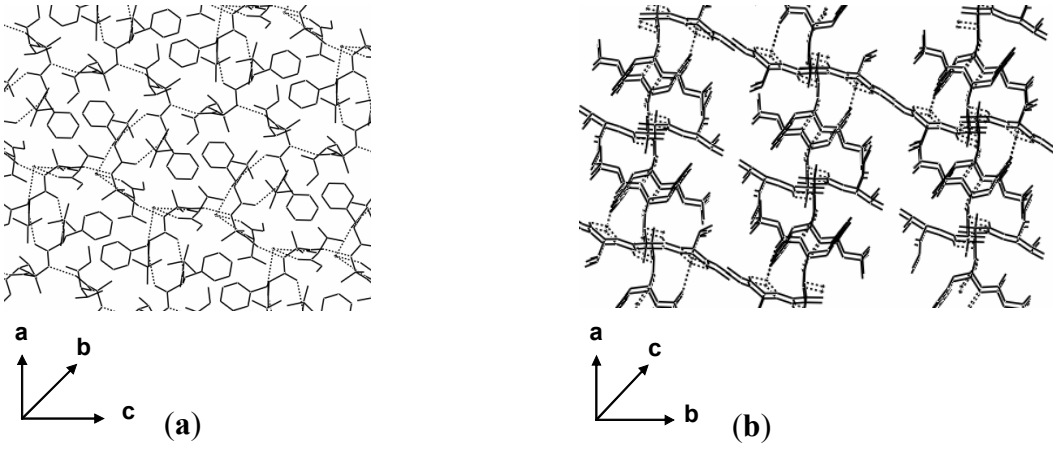

Figure 5. Packing pattern of peptide **1** showing (a) the formation of β-sheet layer in the *ac* plane. Only intermolecular hydrogen bonds are shown with dotted lines; (b) the formation of supramolecular β-sheet through the higher order self-assembly of layers in the *b* direction.

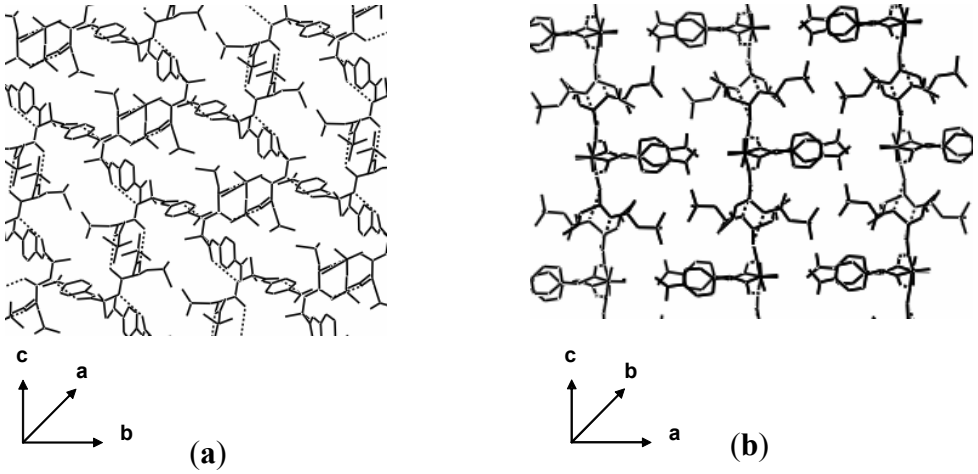

Figure 6. Packing pattern of peptide **2** showing (a) the formation of β-sheet layer in *bc* plane. Only intermolecular hydrogen bonds are shown with dotted lines; (b) the formation of supramolecular β-sheet through the higher order self-assembly of layers in *a* direction.

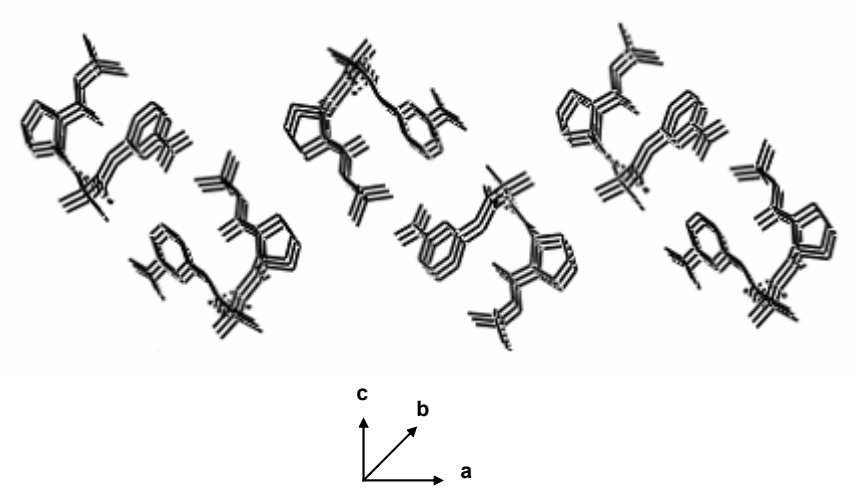

Figure 7. Packing pattern of peptide **3** showing the formation of semicylindrical structures in the *b* direction. The cylindrical structures are packed through van der Waals interactions to form layers of β-turns in the *ac* plane.

Peptide conformations in solution

The solution phase conformation of the peptide **1** was probed by NMR solvent titration method. In this experiment a solution of the peptide **1** in nonpolar $CDCl_3$ (10 mM in 0.5 ml) was gradually titrated against polar $(CD_3)_2SO$ and the changes in the chemical shifts of NHs were recorded by ^1H NMR (Fig. 8).[26] The solvent titration shows that by increasing the percentage of $(CD_3)_2SO$ in $CDCl_3$ from 0 to 10% the net changes in the chemical shift (Δδ) values for Phe(1)-NH, Aib(2)-NH and Val(3)-NH are 0.94, 0.84 and 0.10 ppm, respectively. The Δδ values demonstrate that Val(3)-NH is solvent shielded, and the other two NH groups are solvent exposed, which is a characteristic feature of a turn-like structure where the Val(3)-NH is involved in an intramolecular hydrogen bond to Boc-CO. Although peptide **1A** and **1B** do not form any intramolecular hydrogen bond in crystal structure (Fig. 2), in the solution phase they build up intramolecular 4→ 1 hydrogen bond. The CD spectrum of peptide **1** at 25^0C in methanol reveals a positive ellipticity in the far-UV region with distinct double maxima at 206 and 222 nm, suggesting the presence of a turn structure (Fig. 9).[27]

In ^1H NMR solvent titration of peptide **2** the net change in the chemical shift (Δδ) values for Leu(1)-NH, Aib(2)-NH and *p*-NA(3)-NH are 1.03, 0.93 and 0.00 ppm, respectively (Fig. 10), indicating a turn-like structure where *p*-NA(3)-NH is hydrogen bonded to Boc-CO. Interestingly the crystal structure of **2** does not contain any intramolecular 4→ 1 hydrogen bond (Fig. 4). The CD spectra of peptide **2** in methanol displays a strong positive ellipticity in the far-UV region with a distinct maxima at 199 nm (Fig. 9), which indicates the presence of a turn structure.

The solvent dependence of the NH chemical shifts, that is demonstrated in this $CDCl_3$-$(CD_3)_2SO$ titration experiment, indicates that Aib(2)-NH is free and *m*-NA(3)-NH is hydrogen bonded in peptide **3** with Δδ values as 0.97 and -0.06 ppm respectively, indicating a β-turn structure (Fig.

11). A positive ellipticity with a maxima at 197 nm is observed in the CD spectra of **3** in methanol (Fig. 9), indicating the population of β-turn structure. Therefore, the results of solvent dependent NMR titrations and CD spectroscopy strongly favor the conclusion that the peptides **1-3** are folded into turn structures in the solution phase.

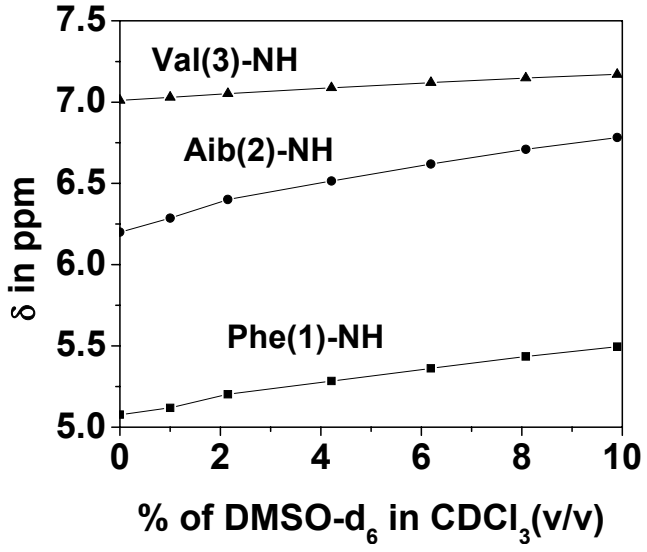

Figure 8. NMR solvent titration curve for NH protons in peptide **1**.

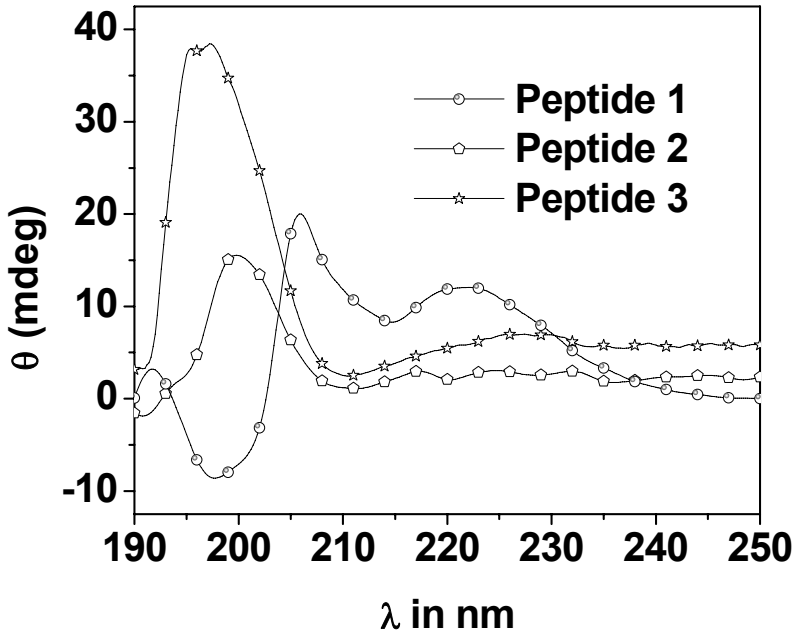

Figure 9. CD curves of peptides **1-3** in methanol (1.5 mM).

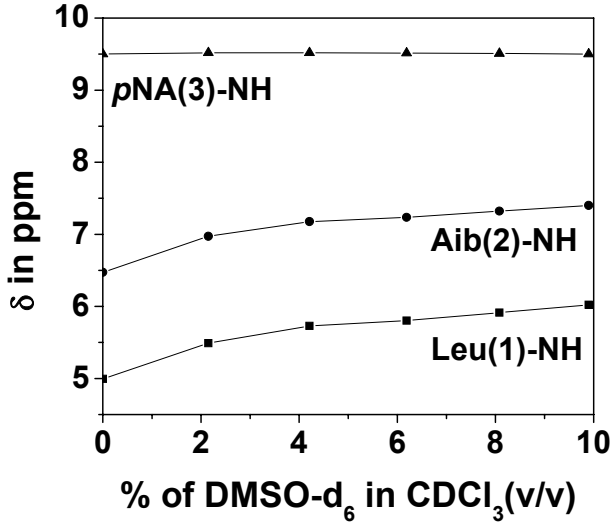

Figure 10. NMR solvent titration curve for NH protons in peptide **2**.

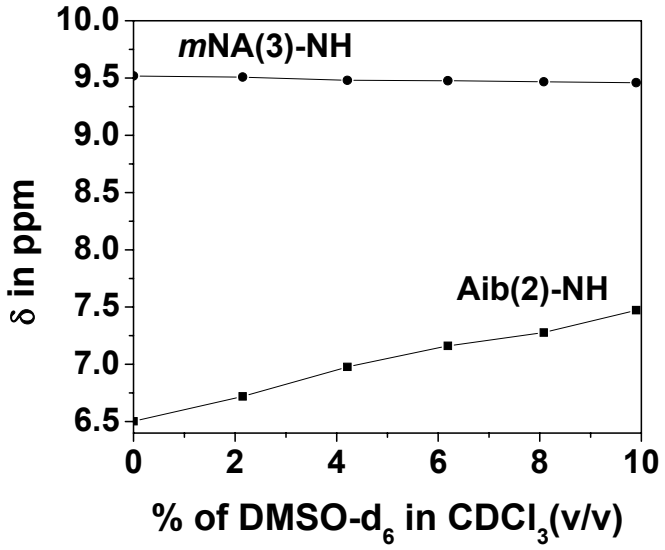

Figure 11. NMR solvent titration curve for NH protons in peptide **3**.

Morphological studies

In addition to naturally occurring amyloid proteins, researchers have studied a variety of other β-sheet fibril-forming motifs derived from amyloid protein fragments, *de novo* designed peptides, peptidomimetics, and peptide amphiphiles. Schneider *et al* have reported the formation of flat fibril laminates through β-sheet mediated self-assembly of peptide with central Pro-Pro fragment.[28] The quasi-crystalline structures of flat and non-twisted morphology are useful for specific nano-applications. Various attempts to fabricate these types of structures using amyloid

proteins, peptides, and viruses have been reported.[29] Therefore we became interested in exploring the possibility of fibril formation in peptides **1**-**3**. Field emission scanning electron microscopic (FE-SEM) images of the dried fibrous material of peptides **1-3** grown slowly from ethylacetate–petroleum ether (for **1**) and acetone (for **2** & **3**) clearly demonstrate that the aggregates in the solid state are bunches of fibrillar structures of flat morphology (Fig. 12a-c). The fibrillar structures are formed through β-sheet mediated self-assembly of the preorganized turn-like building blocks.

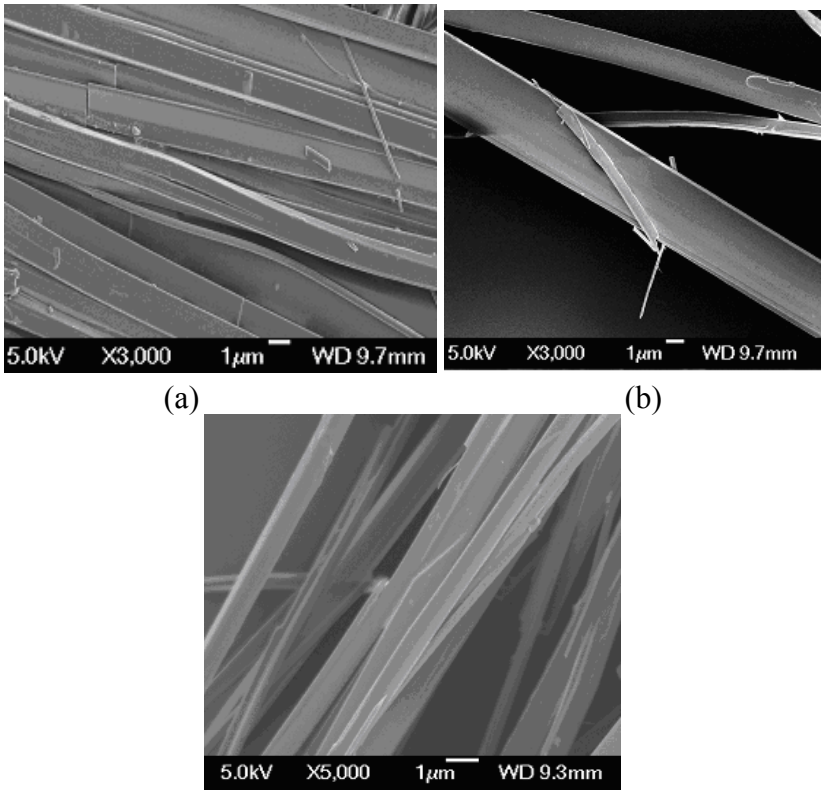

(a) (b)

(c)

Figure 12. FE-SEM images of (a) peptide **1**, (b) peptide **2** and (c) peptide **3** showing the formation of fibrillar structures of flat morphology in the solid state. The fibrous materials of peptide **1** was grown slowly from ethylacetate-petroleum ether and peptide **2** and **3** from acetone. They were dried and gold coated.

Conclusions

The present studies show that the turn-like structures of peptides **1**-**3** are quite stable and exist both in the solid state and in solution. Due to the presence of flat aromatic rings in the backbones these turn structures show a high tendency to form supramolecular β-sheets through molecular self-assembly. It has been shown that these preorganized turn building blocks generate flat fibrillar structures through β-sheet mediated self-assembly. The importance of π-π interactions in

the formation of amyloid fibrils has been documented previously.[30] The present study provides useful insights about the design and self-assembly of peptides, specifically, the relationship between peptide structure and the consequent morphology of the self-assembled materials.

Experimental Section

Synthesis of the peptides

The peptides were synthesized by conventional solution phase methods. The t-butyloxycarbonyl (Boc) group was used for N-terminal protection and the C-terminus was protected as the methyl ester. Couplings were mediated by dicyclohexylcarbodiimide (DCC)/ 1-hydroxybenzotriazol (HOBT). All intermediates were characterized by thin layer chromatography on silica gel and used without further purification. Final peptides were purified by column chromatography using silica gel (100-200 mesh) as the stationary phase. Ethylacetate and petroleum ether mixture was used as the eluent. The reported peptides **1-3** were fully characterized by X-ray crystallography and NMR studies.

Synthesis of the peptide 1, Boc-Phe-Aib-Val-OMe

Peptide Boc-Phe-Aib-OH[22(e)] (2.30g, 6.60 mmol) was dissolved in dimethylformamide (DMF, 10 ml). Val-OMe obtained from its hydrochloride (2.20g, 13.00 mmol) was added to the former solution in ice-cold condition followed by addition of DCC (2.00g, 9.70 mmol). The reaction mixture was stirred at room temp. for 2 days. The precipitated dicyclohexylurea (DCU) was filtered off. The filtrate was diluted with ethylacetate. The organic layer was washed with 1N HCl (3 x 30 ml), brine, 1M Na_2CO_3 solution (3 x 30 ml) and again with brine. The solvent was then dried over anhydrous Na_2SO_4 and evaporated in *vacuo* giving a light yellow gum. Yield: 2.50g (82.20 %). Single crystals were grown from ethylacetate-petroleum ether solvent by slow evaporation and were stable at room temp. Mp= 94^0C. Anal.Calcd for $C_{24}H_{37}N_3O_6$ (463.55): C, 62.17; H, 8.04; N, 9.06. Found: C, 62.22; H, 8.09; N, 9.11%. $[\alpha]_{589}^{20}$ = -28 ^{0} (c = 0.10 g per 100 ml; CH_3OH); IR (KBr): 3330, 3305, 2972, 1704, 1662, 1532 cm^{-1}; ^{1}H NMR 300 MHz ($CDCl_3$, δ ppm): 7.25-7.34 (Phenyl ring protons), 7.01 (Val-NH, 1H, *d*), 6.20 (Aib -NH, *s*), 5.07 (Phe-NH, 1H, *s*), 4.45-4.50 ($C^{\alpha}H$ of Val, 1H, *m*), 4.24 ($C^{\alpha}H$ of Phe, 2H, *m*), 3.72(-OCH_3 , 3H, *s*), 3.04 –3.08($C^{\beta}H$ of Phe, 2H, *m*), 2.16-2.18 ($C^{\beta}H$ of Val, 1H, *m*), 1.61 (Boc-CH_3 s, 9H, *s*), 1.45 and 1.50 ($C^{\beta}H$ of Aib, 6H, *s*), 0.89-0.97 ($C^{\gamma}H$ of Val, 6H, *m*); HR-MS (M^+Na^+) =485.975, M_{calcd} $(M^+Na)^+$ = 486.55.

Synthesis of the peptide 2, Boc-Leu-Aib-*p*-NA

Peptide Boc-Leu-Aib-OH[22c] (1.00g, 3.16 mmol**)** was dissolved in 5 ml of DMF. *para*-Nitroaniline (0.86 g, 6.32 mmol) was added to the former solution in ice-cold condition followed by addition of DCC (0.98g, 4.74 mmol) and HOBT (0.43 g, 3.16 mmol). The reaction mixture was stirred at room temp for 2 days .The precipitated DCU was filtered off. The filtrate was

diluted with ethylacetate. The organic layer was washed with 1N HCl (3x30 ml) brine, 1M Na_2CO_3 solution (3x30 ml) and again with brine. The solvent was then dried over anhydrous Na_2SO_4 and evaporated in *vacuo* giving a light yellow gum. Yield: 1.2g (86.95%). The peptide was purified by column chromatography using 20% ethylacetate-petroleum ether gradient. Single crystals were grown from acetone by slow evaporation and were stable at room temp. Mp= 174^0C. Anal.Calcd for $C_{21}H_{32}N_4O_6$ (436.50): C, 57.77; H, 7.38; N, 12.83. Found: C, 57.68; H, 7.31; N, 12.73 %. $[\alpha]_{589}^{20}$ = -20 ^{0} (c = 0.10 g per 100 ml; CH_3OH); IR (KBr): 3754.1, 3324.2, 3259.6, 2953, 2868.3, 1674.3, 1602.9, 1524, cm^{-1}; ^{1}H NMR 300 MHz ($CDCl_3$, δ ppm): 9.50 (*p*NA(3)-NH, 1H, *s*), 8.17(H_a *p*NA(3), 2H, *d*, *J*=5.1Hz), 7.89 (H_b *p*NA(3), 2H, *d*, *J*=9Hz), 6.36(Aib(2)-NH, 1H, *s*), 4.96(Leu(1)-NH,1H, *s*), 3.92($C^{\alpha}H$ of Leu(1), 1H, *m*), 1.57 & 1.55($C^{\beta}H$ of Aib(2), 6H, *s*),1.25($C^{\beta}H$ of Leu(1), 2H, *m*), 1.46 (Boc-CH_3 s, 9H, *s*), 0.97(C^{γ} and $C^{\delta}H$ of Leu(1), 7H, *m*). ^{13}C NMR 75MHz ($CDCl_3$, δ ppm): 172.81, 171.8, 144.80, 124.76, 119.50, 81.44, 54.76, 40.12, 28.26, 26.10, 25.11, 24.90, 22.89, 21.76; HR-MS (M^+Na^+) = 459.16, M_{calcd} $(M^+Na)^+$ = 459.50.

Synthesis of the peptide 3a, Boc-Pro-Aib-OMe

Boc-Pro-OH (2.0g, 9.30 mmol) was dissolved in a mixture of dichloromethane (DCM, 6 ml) and dimethylformamide (DMF, 2 ml). Aib-OMe obtained from its hydrochloride (2.85g, 18.6 mmol) was added to the former solution followed by addition of DCC (2.87g, 13.95 mmol) in ice-cold condition. The reaction mixture was stirred at room temp. for 1 day. The precipitated dicyclohexylurea (DCU) was filtered off. The filtrate was diluted with ethylacetate. The organic layer was washed with 1N HCl (3x30 ml), brine, 1M Na_2CO_3 solution (3x30 ml) and then again with brine. The solvent was dried over anhydrous Na_2SO_4 and evaporated in *vacuo*, giving a light yellow gum. Yield: 2.5g (86%).

Synthesis of the peptide 3b, Boc-Pro-Aib-OH

Peptide **3a** (2.5g, 7.96 mmol) was dissolved in methanol (20 ml) and 2N NaOH (10 ml) was added to it. The reaction mixture was stirred for 1 day at room temperature. The progress of reaction was monitored by TLC. After completion of reaction the methanol was evaporated. The residue was diluted with water and washed with diethylether. The aqueous layer was cooled on ice, neutralized by using 2N HCl and extracted with ethylacetate. The solvent was evaporated in *vacuo* to give a waxy white coloured solid. Yield: 2.1g (88%).

Synthesis of the peptide 3, Boc-Pro-Aib-*m*-NA

Peptide **3b** (2.1g, 7.00 mmol) was dissolved in dichloromethane (DCM, 5ml). *meta*-Nitroaniline (1.93g, 14 mmol) was added to former solution, followed by addition of DCC (2.16g, 10.5 mmol) in ice-cold condition. The reaction mixture was stirred at room temp for 2 days. The precipitated dicylohexylurea (DCU) was filtered off. The filtrate was diluted with ethylacetate. The organic layer was washed with 1N HCl (3x30ml), brine, 1M Na_2CO_3 solution (3x30 ml) and then again with brine. The solvent was then dried over anhydrous Na_2SO_4 and evaporated in *vacuo*, to give a white solid compound. Purification was done using silica gel as stationary phase

and ethylacetate-petroleum ether mixture (1:4) as eluent. Single crystals were grown from acetone by slow evaporation and were stable at room temp. Yield: 3.0g (76.92%). Mp= 122^{0}C; Anal.Calcd for $C_{20}H_{28}N_4O_6$ (420.34): C, 57.14; H, 6.68; N, 13.33%; Found: C, 57.05; H, 6.59; N, 13.25%. $[\alpha]_{589}^{20}$ = -18 ^{0} (c = 0.10 g per 100 ml; CH_3OH); IR (KBr): 3754.2, 3689.7, 3315.9, 2979.6, 2934.7, 1670.6, 1534.3 cm^{-1}; ^{1}H NMR 300 MHz ($CDCl_3$, δ ppm): 9.51(*m*NA(3)-NH, 1H, *s*), 8.57(H_a *m*NA(3), 1H, *s*), 8.21(H_d *m*Na(3), 1H, *d*, *J*=7.2Hz), 7.90(H_b *m*ABA(3), 1H, *d*, *J*=6Hz), 7.43(H_c *m*NA(3), 1H, *t*, *J*=8.1Hz), 6.50(Aib(2)-NH, 1H, *s*), 4.15($C^{\alpha}H$ of Pro(1), 1H, *m*), 3.50($C^{\gamma}H$ of Pro(1), 2H, *m*), 2.23($C^{\beta}H$ of Pro(1), 2H, *m*), 1.98 ($C^{\delta}H$ of Pro(1), 2H, *m*), 1.46 (Boc-CH_3 s, 9H, *s*), 1.64 & 1.57($C^{\beta}H$ of Aib(2), 6H, *s*); ^{13}C NMR 75MHz ($CDCl_3$, δ ppm):156.2,148.44, 140.05, 129.35, 125.83, 118.21,115.01, 81.37, 61.48, 57.90, 51.99, 47.41, 30.84, 29.64, 28.28, 26.53, 24.99, 24.62; HR-MS (M^+Na^+) = 443.20, M_{calcd} $(M^+Na)^+$ = 443.34.

FT-IR spectroscopy

IR spectra were examined using a Perkin Elmer-782 model spectrophotometer. The solid- state FT-IR measurements were performed using the KBr disk technique.

NMR experiments

All ^{1}H NMR and ^{13}C NMR spectra of peptides **1-3** were recorded on a Bruker Avance 300 model spectrometer operating at 300, 75 MHz respectively. The peptide concentrations were 10 mM in $CDCl_3$ for ^{1}H NMR and 40 mM in $CDCl_3$ for ^{13}C NMR. Solvent titration experiments were carried out at a concentration of 10 mM in $CDCl_3$ with gradual addition of d_6-DMSO from 0-10% v/v approximately.

Circular Dichroism spectroscopy

Solutions of peptides **1-3** in MeOH (1.5 mM as final concentration) were used for obtaining the spectra. Far-UV CD measurements were recorded at 25^{o}C with a 0.5 sec averaging time, a scan speed of 50 nm/min, using a JASCO spectropolarimeter (*J* 720 model) equipped with a 0.1 cm pathlength cuvette. The measurements were taken at 0.2 nm wavelength intervals, 2.0 nm spectral bandwidth and five sequential scans were recorded for each sample.

Field Emission scanning electron microscopic study

The morphology of peptides **1-3** was investigated using field emission scanning electron microscope (FE-SEM). For the study, fibrous materials of peptide **1** were slowly grown from ethylacetate-petroleum ether and of peptide **2** and **3** were slowly grown from acetone and then dried and gold coated. The micrographs were taken using a FE-SEM apparatus (JEOL JSM - 6700F).

Mass spectrometry

Mass spectra of peptides **1-3** were recorded on HEWLETT PACKARD Series 1100MSD and Micromass Qtof Micro YA263 Mass spectrometers by positive mode electro spray ionization.

Table 3. Crystallographic refinement details for peptides **1**-**3**

	Peptide **1**	Peptide **2**	Peptide **3**
Crystal Colour	Colourless	Colourless	Colourless
Chemical Formula	$C_{24}H_{37}N_3O_6$, $0.25H_2O$	$C_{21}H_{32}N_4O_6$	$C_{20}H_{25}N_4O_6$
Crystallising solvent	Ethylacetate Petroleum ether	Acetone	Acetone
Formula Weight (g)	469.08	436.51	417.44
Crystal System	monoclinic	orthorhombic	orthorhombic
Space group	$P2_1$	Pbcn	$P2_12_12$
Z	4	8	4
a (Å)	13.6336(6)	19.1499(15)	28.9256(13)
b (Å)	10.8373(4)	10.8592(8)	13.1584(5)
c (Å)	18.4668(7)	23.396(2)	5.7929(2)
β (^{o})	107.361(4)	(90)	(90)
V (Å^3)	2604.19(18)	4865.2(7)	2204.86(15)
Temperature (K)	150(2)	150(2)	150(2)
Unique reflections	12531	7088	6422
Nº Parameters	620	287	276
GoF	1.079	1.093	0.926
R_1 [I>2σ(I)]	0.0518	0.0756	0.0554
wR_2 [I>2σ(I)]	0.1137	0.2382	0.1203

Single crystal X-ray diffraction study

Crystal data and refinement details are given in Table 3. Diffraction data for the three peptides **1**, **2** and **3**, were obtained with MoKα radiation at 150K using the Oxford Diffraction X-Calibur CCD System. The crystals were positioned at 50 mm from the CCD. 321 frames were measured with a counting time of 10 s. Data analyses were carried out with the Crysalis program.[31] The structures were solved using direct methods with the Shelxs97 program.[32] The non-hydrogen atoms were refined with anisotropic thermal parameters. The hydrogen atoms bonded to carbon and nitrogen were included in geometric positions and given thermal parameters equivalent to 1.2 times (1.5 times for methyl hydrogens) those of the atom to which they were attached. Crystallographic details have been deposited at the Cambridge Crystallographic Data centre, reference CCDC 734094 – 734096 inclusive.

Acknowledgements

S.K. thanks CSIR, New Delhi, India, for a Senior Research Fellowship (SRF). The financial assistance of UGC, New Delhi is acknowledged [Major Research Project, No.32-190/2006(SR)]. We acknowledge the financial assistance of Centre for Research in Nanoscience & Nanotechnology, University of Calcutta. We thank EPSRC and the University of Reading, UK for funds for Oxford Diffraction X-Calibur CCD diffractometer.

References and Notes

1. Maji, S. K.; Banerjee, A.; Drew, M. G. B.; Halder, D.; Banerjee, A. *Tetrahedron Lett.* **2002**, *43*, 6759.
2. Halder, D.; Maji, S. K.; Drew, M. G. B.; Banerjee, A. *Tetrahedron Lett.* **2002**, *43*, 5465.
3. Maji, S. K.; Drew, M. G. B.; Banerjee, A. *Chem. Commun.* **2001**, 1946-1947.
4. Vauthey, S.; Santoso, S.; Gong, H.; Watson, N.; Zhang, S. *Proc. Natl. Acad. Sci. USA* **2002**, *99*, 5355.
5. Rathore, O.; Sogah, D. Y. *J. Am. Chem. Soc.* **2001**, *123*, 5231.
6. Caplan, M. R.; Moore, P. N.; Zhang, S.; Kamm, R. D.; Lauffenburger, D. A. *Biomacromolecules* **2000**, *1*, 627.
7. Krejchi, M. T.; Atkins, E. D. T.; Waddon, A. J.; Fournier, M. J.; Mason, T. L.; Tirrel, D. A. *Science* **1994**, *265*, 1427.
8. Wang, W.; Hecht, M. H. *Proc. Natl. Acad. Sci. USA* **2002**, *99*, 2760.
9. Antzutkin, O. N.; Balbach, J. J.; Leapman, R. D.; Rizzo, N. W.; Reed, J.; Tycko, R. *Proc. Natl. Acad. Sci. USA* **2000**, *97*, 13045.
10. Tjernberg, L. O.; Callway, D. J. E.; Tjernberg, A.; Hahne, S.; Lilliehöök, C.; Terenius, L.; Thyberg, J.; Nordsted, C. *J. Biol. Chem.* **1999**, *274*, 12619.
11. Benzinger, T. L. S.; Gregory, D. M.; Burkoth, T. S.; Miller-Auer, H.; Lynn, D. G.; Botto, R. E.; Maredith, S. C. *Proc. Natl. Acad. Sci. USA* **1998**, *95*, 13407.
12. Dutt, A.; Drew, M. G. B.; Pramanik, A. *Org. Biomol. Chem.* **2005**, *3*, 2250.
13. Kundu, S. K.; Majumder, P. A.; Das, A. K.; Bertolasi, V.; Pramanik, A. *J. Chem. Soc. Perkin Trans.* **2002**, *2*, 1602.
14. Maji, S. K.; Haldar, D.; Drew, M. G. B.; Banerjee, A.; Das, A. K.; Banerjee, A. *Tetrahedron* **2004**, *60*, 3251.
15. Banerjee, A.; Maji, S. K.; Drew, M. G. B.; Haldar, D.; Banerjee, A. *Tetrahedron Lett.* **2003**, *44*, 335.
16. Halder, D.; Maji, S. K.; Sheldrick, W. S.; Banerjee, A. *Tetrahedron Lett.* **2002**, *43*, 2653.
17. Kar, S.; Dutta, A.; Drew M. G. B.; Koley, P. Pramanik, A. *Supramolecular Chemistry* DOI**:** 10.1080/10610270802709378.

18. Lashuel, H. A.; LaBrenz, S. R; Woo, L; Serpell, L. C.; Kelly, J. W. *J. Am. Chem. Soc.* **2000**, *122*, 5262.
19. (a) Venkatraman, J.; Shankaramma, S. C.; Balaram, P. *Chem Rev*. **2001**, *101*, 3131. (b) Andreeto, E.; Peggion, C.; Crisma, M.; Toniolo, C. *Biopolymers* **2006**, *84*, 490. (c) Rai, R.; Aravinda. S.; Kanagarajadurai, K.; Raghothama, S.; Shamala, N.; Balaram, P. *J. Am. Chem. Soc*. **2006**, *128*, 7916. (d) Crisma, M.; Andreeto, E.; Zotti, M. D.; Moretto, A.; Peggion, C.; Formaggio, F.; Toniolo, C. *J. Pept. Sci.* **2007**, *13*, 190.
20. Maji, S. K.; Malik, S.; Drew, M. G. B.; Nandi, A. K.; Banerjee, A. *Tetrahedron Lett.* **2003**, *44*, 4103.
21. Maji, S. K.; Drew, M. G. B.; Banerjee, A. *Chem. Commun*. **2001**, 1946.
22. (a) Dutt, A.; Dutta, A.; Mondal, R.; Spencer, E. C.; Howard, J. A. K.; Pramanik, A. *Tetrahedron* **2007**, *63*, 10282. (b) Halder, D.; Drew, M. G. B.; Banerjee, A. *Tetrahedron* **2007**, *63*, 5561. (c) Dutt, A.; Drew, M. G. B.; Pramanik, A. *Tetrahedron* **2005**, *61*, 11163. (d) Das, A. K.; Banerjee, A.; Drew, M. G. B.; Ray, S.; Haldar, D.; Banerjee, A. *Tetrahedron* **2005**, *61*, 5027. (e) Dutt, A.; Frohlick, R.; Pramanik, A.; *Org. Biomol. Chem.* **2005**, *3*, 661. (f) Banerjee, A.; Maji, S. K.; Drew, M. G. B.; Haldar, D.; Banerjee, A. *Tetrahedron Lett.* **2003**, *44*, 6741.
23. Lee, H. B.; Zaccaro, M. C.; Pattarawarapan, M.; Roy, S.; Saragovi, H. B.; Burgess, K. *J. Org. Chem.* **2004**, *69*, 701.
24. Venkatachalam, C. M. *Biopolymers* **1968**, *6*, 1425.
25. (a) Dutt, A.; Drew, M. G. B.; Pramanik, A. *Tetrahedron*, **2005**, *61*, 11163. (b) Crisma, M.; Valle, G.; Toniolo, C.; Prasad, S.; Rao, R. B.; Balaram, P.; *Biopolymers* **1995**, *35*, 1.
26. (a) Banerjee, A.; Raghothama, S.; Balaram, P. J. *Chem. Soc. Perkin Trans.* **1997**, *2*, 2087. (b) Karle, I. L.; Banerjee, A.; Bhattacharya, S.; Balaram, P. *Biopolymers* **1996**, *38*, 515.
27. Prasad, S.; Rao, R. B.; Balaram, P. *Biopolymers* **1994**, *35*, 11.
28. Lamm, M. S.; Rajagopal, K.; Schneider, J. P.; Pochan, D. J. *J. Am. Chem. Soc.* **2005**, *127*, 16692.
29. (a) Sone, E. D.; Stupp, S. I. *J. Am. Chem. Soc.* **2004**, *126*, 12756. (b) Meegan, J. E.; Aggeli, A.; Boden, N.; Brydson, R.; Brown, A. P.; Carrick, L.; Brough, A. R.; Hussain, A.; Ansell, R. J. *Adv. Funct. Mater.* **2004**, *14*, 31. (c) Mao, C.; Flynn, C. E.; Hayhurst, A.; Sweeney, R.; Qi, J.; Georgiou, G.; Iverson, B.; Belcher, A. M. *Proc. Natl. Acad. Sci. U. S. A.* **2003**, *100*, 6946. (d) Scheibel, T.; Parthasarathy, R.; Sawicki, G.; Lin, X. M.; Jaeger, H.; Lindquist, S. L. *Proc. Natl. Acad. Sci. U. S. A*. **2003**, *100*, 4527. (e) McMillan, R. A.; Paavola, C. D.; Howard, J.; Chan, S. L.; Zaluzec, N. J.; Trent, J. D. *Nat. Mater.* **2002**, *1*, 247. (f) Hartgerink, J. D.; Beniash, E.; Stupp, S. I. *Science* **2001**, *294*, 1684. (g) Shenton, W.; Douglas, T.; Young, M.; Stubbs, G.; Mann, S. *Adv. Mater.* **1999**, *11*, 253.
30. Gazit, E. *J. FASEB* **2002**, *16*, 77.
31. Crysalis, v1 (**2005**) Oxford Diffraction Ltd., Oxford, U.K.
32. G. M. Sheldrick, SHELXS-97 and SHELXL-97, Programs for Crystal Structure solution and determination, University of Göttingen: Göttingen, Germany, **1997**.